(2) LEVEL III

IDA PAPER P-1465

INTERNAL WAVE INDUCED MAGNETIC FIELD AND MAGNETIC FIELD GRADIENT SPECTRA AS WOULD BE MEASURED BY AN AIRBORNE MAGNETIC SENSOR

Wasyl Wasylkiwskyj
Elaine Marcuse

May 1980

Prepared for
Defense Advanced Research Projects Agency

IDA
INSTITUTE FOR DEFENSE ANALYSES
SCIENCE AND TECHNOLOGY DIVISION

IDA Log No. HQ 80-22011

The work reported in this document was conducted under contract MDA 903 79 C 0202 for the Department of Defense. The publication of this IDA Paper does not indicate endorsement by the Department of Defense, nor should the contents be construed as reflecting the official position of that agency.

UNCLASSIFIED

SECURITY CLASSIFICATION OF THIS PAGE (When Data Entered)

REPORT DOCUMENTATION PAGE		READ INSTRUCTIONS BEFORE COMPLETING FORM
1. REPORT NUMBER	2. GOVT ACCESSION NO. AD-A089 645	3. RECIPIENT'S CATALOG NUMBER
4. TITLE (and Subtitle) Internal Wave Induced Magnetic Field and Magnetic Field Gradient Spectra as Would Be Measured by an Airborne Magnetic Sensor		5. TYPE OF REPORT & PERIOD COVERED FINAL
		6. PERFORMING ORG. REPORT NUMBER IDA Paper P-1465
7. AUTHOR(s) W. Wasylkiwskyj		8. CONTRACT OR GRANT NUMBER(s) MDA 903 79 C 0202
9. PERFORMING ORGANIZATION NAME AND ADDRESS Institute for Defense Analyses 400 Army-Navy Drive Arlington, Virginia 22202		10. PROGRAM ELEMENT, PROJECT, TASK AREA & WORK UNIT NUMBERS DARPA Assignment A-49
11. CONTROLLING OFFICE NAME AND ADDRESS Defense Advanced Research Projects Agency 1400 Wilson Boulevard Arlington, Virginia 22209		12. REPORT DATE May 1980
		13. NUMBER OF PAGES 45
14. MONITORING AGENCY NAME & ADDRESS(if different from Controlling Office)		15. SECURITY CLASS. (of this report) UNCLASSIFIED
		15a. DECLASSIFICATION DOWNGRADING SCHEDULE —

16. DISTRIBUTION STATEMENT (of this Report)

Approved for public release; distribution unlimited.

17. DISTRIBUTION STATEMENT (of the abstract entered in Block 20, if different from Report)

None

18. SUPPLEMENTARY NOTES

N/A

19. KEY WORDS (Continue on reverse side if necessary and identify by block number)

electromagnetic fields of ocean currents; magnetic anomaly detection; spectra of ocean internal waves; magnetic field gradients; electromagnetic fields induced by conducting fluids; magnetohydrodynamic phenomena

20. ABSTRACT (Continue on reverse side if necessary and identify by block number)

A technique is described for computing internal wave induced magnetic field and magnetic field gradient spectra as these would be measured by airborne magnetic sensors. The intended application is remote sensing of internal wave activity in the upper layers of a deep ocean in the wavelength range less that 1 km. A computer program (INTWAVE) is presented which is capable of accepting data from towed thermistor chain measurements. Numerical results obtained with INTWAVE

DD FORM 1 JAN 73 1473 EDITION OF 1 NOV 65 IS OBSOLETE

UNCLASSIFIED

SECURITY CLASSIFICATION OF THIS PAGE (When Data Entered)

20.

are presented for the measured internal wave spectra reported by Nelson and Milder [4].

IDA PAPER P-1465

INTERNAL WAVE INDUCED MAGNETIC FIELD AND MAGNETIC FIELD GRADIENT SPECTRA AS WOULD BE MEASURED BY AN AIRBORNE MAGNETIC SENSOR

Wasyl Wasylkiwskyj
Elaine Marcuse

May 1980

INSTITUTE FOR DEFENSE ANALYSIS
SCIENCE AND TECHNOLOGY DIVISION
400 Army-Navy Drive, Arlington, Virginia 22202

Contract MDA 903 79 C 0202
DARPA Assignment A-49

ABSTRACT

A technique is described for computing internal wave induced magnetic field and magnetic field gradient spectra as these would be measured by airborne magnetic sensors. The intended application is remote sensing of internal wave activity in the upper layers of a deep ocean in the wavelength range less than 1 km. A computer program (INTWAVE) is presented which is capable of accepting data from towed thermistor chain measurements. Numerical results obtained with INTWAVE are presented for the measured internal wave spectra reported by Nelson and Milder [4].

CONTENTS

FIGURES

I. INTRODUCTION

The subject of this paper is the determination of internal wave induced magnetic field and magnetic field gradient spectra as would be measured by a magnetic sensor mounted on an airborne measurement platform. The principal interest is in sensing of internal wave activity in the upper layer of a deep ocean in the wavelength range below 1 km. The theoretical basis of the approach used here has been set forth in [1] in conjunction with the internal wave model developed in [3]. The purpose of the present paper is to describe a systematic technique for computation of magnetic field and magnetic field gradient spectra using as input data measured "towed" spectra of internal wave vertical displacement. The internal wave model underlying the magnetic field spectra calculations is based on the equipartition hypothesis of Milder [3].

In Sections II and III general characteristics of internal wave spectra predicted by this model are summarized and the physical constants and ocean stratifications considered in the calculations are presented. Section IV provides the analytical relationships between the internal wave parameters and the magnetic field and magnetic field gradient spectra for airborne observation platforms.

A general computer program (INTWAVE) capable of providing the spectra for rather general deep ocean Väisälä frequency profiles is described in detail in the Appendix. The input data can be either in the form of analytic expressions or supplied in numerical form.

Representative results obtained with INTWAVE are plotted in Figs. 3-8. Figures 3 and 4 give magnetic field gradient spectra for the exponential thermocline described by Garrett and Munk [2]. Figures 5-8 are based on the measured data as reported by Nelson and Milder [4], the Väisälä frequency profile for which is plotted in Fig. 1 (labeled case 4, STD data).

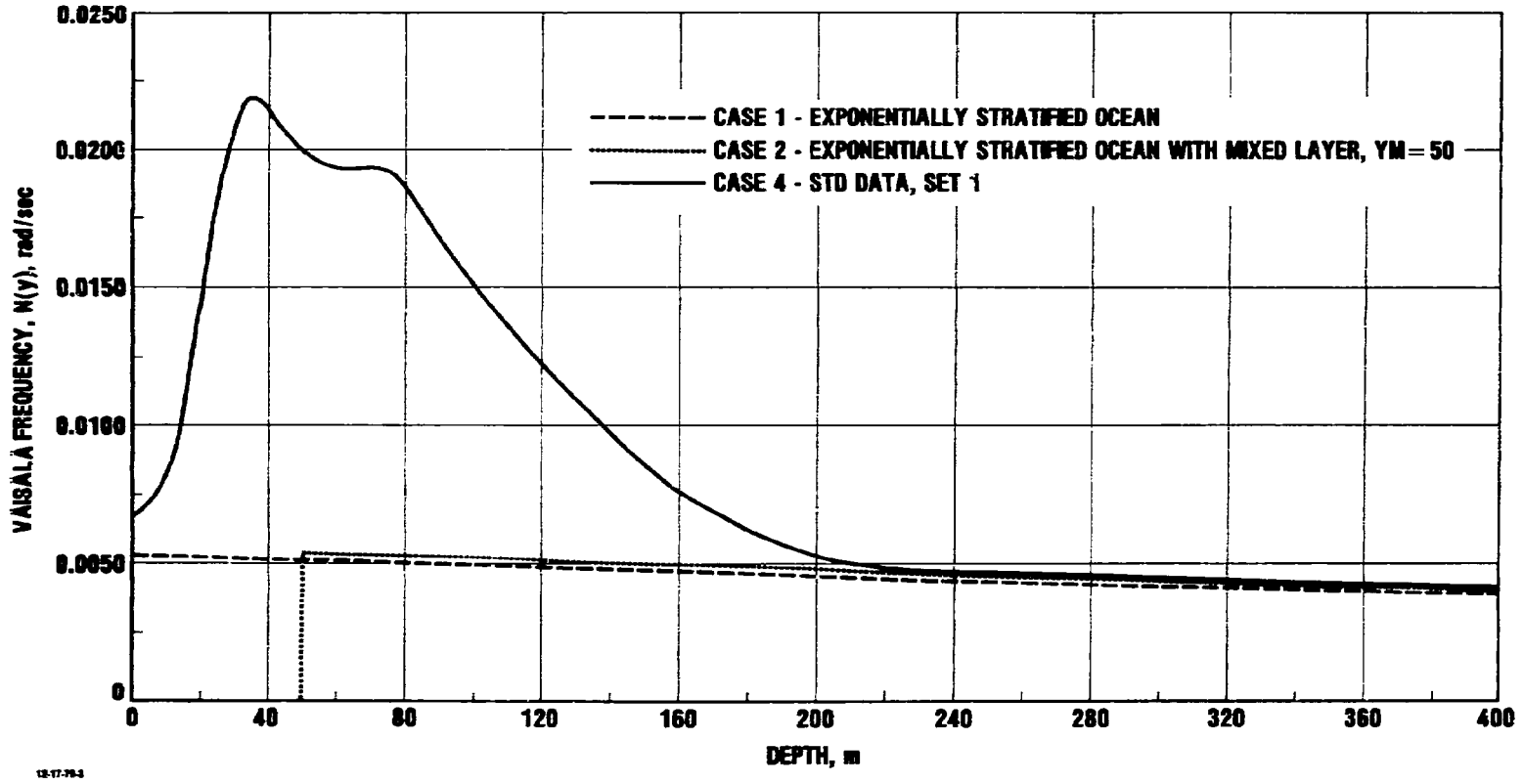

FIGURE 1. Väisälä Frequency Profiles Used in the Calculation of Magnetic Field Gradient Spectra

II. THE INTERNAL WAVE MODEL

The model adopted herein for internal waves in the upper layers of a deep ocean is based on linearized dynamics under conditions of vanishing mean shear flow. The statistical description leading to analytical representations of temporal and spatial spectra utilizes the usual assumptions of spatial and temporal stationarity as employed, e.g., by Garrett and Munk [2]. The interest here is in detection of internal wave phenomena in the frequency range $\omega > 0.5\ N_{max}$ (ω = radian frequency, N_{max} = max Väisälä frequency), i.e., in the so-called buoyancy range. In this range the results of [2] are not directly applicable.

A theory which focuses on the buoyancy range has been advanced by Milder [3]. Milder's theory is based on rather general premises involving conditions of statistical equilibrium. The underlying hypothesis is that of equipartition involving vorticity and strain of the internal wave field. The consequences of this equipartition can be reduced to one remarkably simple rule: the energy content of the normal modes is proportional to the square of the mode phase velocities. It has been shown that in the frequency range $\omega \approx 0.5\ N_{max}$ Milder's theory gives essentially the same results as that of Garrett and Munk [3], [1, p. 265]. The functional form of the spatial spectrum of the isotherm displacement predicted by Milder's theory appears to be in agreement with towed thermistor measurement data reported by Nelson and Milder [4].

Specifically, the equipartition hypothesis leads to the following canonical form of the spatial wave number spectrum for the vertical displacement:

$$KS_{\eta\eta}(K,y) = \frac{I(K)}{2\pi K} \left(1 - e^{-2Ky}\right) \quad , \tag{1}$$

where y (y > 0) is the depth and $K \equiv 2\pi/\lambda$ is the horizontal wavenumber. The spatial wavenumber spectrum $S_{\eta\eta}(K,y)$ is defined such that the statistical average of the square of the internal wave vertical displacement is given by

$$\langle \eta^2 \rangle = 2\pi \int_0^\infty dK \; KS_{\eta\eta}(K,y) \quad . \tag{2}$$

The spectral quantity I(K) depends only on the magnitude of the horizontal wave number so that the spatial spectrum $S_{\eta\eta}(K)$ is isotropic. The most striking feature of (1) is its total independence of the ocean stratification. On the other hand, the spatial spectra of the fluid velocity components depend explicitly on the Väisälä frequency profile N(y). From [1, p. 255] the spatial spectrum of the vertical velocity S_{yy} is given by

$$KS_{yy}(K,y) = \frac{1}{4\pi} I(K) \int_0^\infty dy' \; N^2(y') \left[e^{-K(y+y')} - e^{-K|y-y'|}\right]^2 \quad . \tag{3}$$

Similarly, one can show that the spectra of the two orthogonal horizontal velocity components are

$$KS_{xx}(\underline{K},y) = \frac{\cos^2 w}{4\pi K^2} I(K) \int_0^\infty dy' \; N^2(y') \left\{\frac{\partial}{\partial y}\left[e^{-K(y+y')} - e^{-K|y-y'|}\right]\right\}^2 , \tag{4}$$

$$KS_{zz}(\underline{K},y) = \frac{\sin^2 w}{4\pi K^2} I(K) \int_0^\infty dy' \; N^2(y') \left\{\frac{\partial}{\partial y}\left[e^{-K(y+y')} - e^{-K|y-y'|}\right]\right\}^2 . \tag{5}$$

The spectra of the components of the horizontal velocity are not isotropic but exhibit the characteristic $\cos^2 w$ ($\sin^2 w$) dependence on w, w being the polar angle of $\underline{K}$. On the basis of data in [4] one finds that within a wide range of wavelengths, viz.,

$$60 \text{ m} < \lambda < 1500 \text{ m} \tag{6}$$

the spectral excitation function I(K) has the form

$$I(K) = C_p K^{-p} \quad , \tag{7}$$

where C_p is a constant dependent on the exponent p. The definitions of I(K) in this paper and [1] differ from the definition in [3]. If we denote the I(K) given in [3, Eq. 52, p. 22] by $\hat{I}(K)$, then

$$I(K) = \frac{K}{8\pi^2} \hat{I}(K) \quad . \tag{8}$$

Also, the spectral density S_ζ of the vertical displacement as given by Eq. (52) in [3] is related to the spectral density in (1) by

$$S_{\eta\eta} = \frac{1}{(2\pi)^2} S_\zeta \quad . \tag{9}$$

The relationship (8) can be inferred by comparison of Eq. (5) on page 5 of [3] with Eqs. E-71 and E-73 of [1].

In the calculations presented in Section IV we consider three types of stratifications. These are shown in Fig. 1. The sharply peaked profile identified in the figure as "case 4 - STD data set" is taken from Fig. 3 of [3], which is based on the towed thermistor chain measurements of internal waves in the eastern tropical Pacific Ocean in the early fall of 1974,

as reported in [4]. The real data extends only to about 220 meters. For the purposes of analytical modeling, an exponentially decreasing Väisälä frequency profile of the form exp (- y/1300) (y in meters) is assumed for y > 220 meters. The profiles labeled case 1 and case 2 are those used by Garrett and Munk [2]. In particular, in the exponentially stratified ocean model (case 1), $N(y) = 5.236 \times 10^{-3}$ exp (- y/1300) rad/sec, i.e., no mixed layer is assumed. In case 2, a mixed layer is assumed to a depth of 50 m (i.e., $N(y) = 0$, $0 \leq y < 50$ m); for y > 50 m the same exponential decay law is assumed as in case 1.

For the STD data set, the empirically determined constants C_p and p are given in Eq. (54) on page 23 of [3]. The units employed in [1] and in the magnetic field calculations in Section IV are always m, kg, sec. In particular, the excitation function I(K), as given by (1) (and also in [1]) always has dimensions of m^2, while the wavenumber $K \equiv 2\pi/\lambda$. In Eq. (54) of [3] different units are employed. In addition, private communication with the author of [3] revealed that $\underset{\sim}{k}$ in Eq. (54) of [3] is actually $1/\lambda$ instead of $2\pi/\lambda$ (λ is in km). Taking this into account, as well as the different normalization of the excitation function as shown in (8), the constant C_p to be used in (7) is

$$C_{1.5} = \frac{.12 \times (2\pi)^{2.5}}{10^{1.5} \times 8\pi^2} = 4.756 \times 10^{-3} \text{ (meters)}^{1/2} . \tag{10}$$

Consequently,

$$I(K) = 4.756 \times 10^{-3} K^{-1.5} \quad m^2 . \tag{11}$$

For the exponential profiles, C_p is determined from the energy density constant E and cutoff wavenumber given in [2]. The cutoff wavenumber, K_c, corresponds to the lower truncation

limit in the Garrett and Munk wavenumber spectrum. We express it in terms of the dimensionless quantity ν_c,

$$\nu_c = K_c b = .3267 \tag{12}$$

where b is the depth at which the Väisälä frequency has decayed to 1/e of its maximum value (at the surface or just below the mixed layer). The second fundamental constant is E, the integrated energy density over a water column. The value given in [2] is

$$E = 3.82 \times 10^3 \text{ joules/m}^2 \quad . \tag{13}$$

The two exponential profiles in Fig. 1 can be represented analytically as follows:

$$N(y) = \begin{cases} 0, & 0 \le y \le y_m \\ N_m \exp\left\{(y_m - y)/b\right\} & ; \quad y > y_m \end{cases} \tag{14}$$

where $y_m = 0$ and $y_m = 50$ m correspond, respectively, to case 1 and case 2. The constant C_p is evaluated by integrating the spatial energy spectrum between $K = K_c$ and $K = \infty$, as described on page 266 of [1]. For the general case in (14) the formula for C_p becomes

$$C_p = \frac{E}{\pi \rho_o N_m^2 b^{p+1} f_p(y_m/b)} \quad , \tag{15}$$

where

$$f_p(y_m/b) = \int_{\nu_c}^{\infty} d\nu \, \nu^{-(p+1)} \left[1 - \frac{e^{-2y_m\nu/b}}{1+\nu} \right] \quad , \tag{16}$$

where $\rho_o = 10^3$ kg/m^2 and Γ is the Gamma function. For $y_m = 0$, one finds [1]

$$C_2 = 1.2166 \times 10^{-3}$$

$$C_1 = 1.8727 \times 10^{-2} \text{ m} \quad .$$

When $y_m \neq 0$ the result of the integration in (16) cannot be expressed in terms of tabulated functions. A numerical integration subroutine is incorporated in the general computer program in the Appendix.

Garrett and Munk use $p = 2$ in their paper [2]. In order to show the sensitivity of the results to changes the two extreme values $p = 1$ and $p = 2$ will be considered.

III. RELATIONSHIP BETWEEN EXPERIMENTALLY DETERMINED TOWED SPECTRA AND THE EXCITATION FUNCTION I(K)

References [3] and [4] provide plots of spatial spectra at different depths from which the constants given in (11) are determined. These spectra are identified as "towed spectra", presumably obtained from an analysis of time series as measured by thermistors towed through the water. The detailed steps employed in the process of reducing the measured time series to the spatial spectra are not presented in [3] and [4]. There are several approximations associated with the translation of towed time series data to equivalent spatial spectra, which approximations also have bearing on the interpretation of the results for magnetic field spectra presented in Section IV. The following is a brief discussion of the nature of these approximations.

If we denote the instantaneous vertical displacement at depth y in the water by $\eta(y,\underline{\rho},t)$ (where $\underline{\rho}$ denotes the horizontal coordinates), the temporal spectrum $\Phi_{\eta\eta}^{(U)}(y,\omega)$ observed in the water at a point moving with horizontal velocity $\underline{U}$ may be defined formally by the relationship

$$\Phi_{\eta\eta}^{(U)}(y,\omega) = \lim_{T \to \infty} \frac{1}{T} \left\langle \left| \int_{-T/2}^{T/2} e^{-i\omega t}\, \eta(y,\underline{U}t,t)\, dt \right|^2 \right\rangle . \qquad (17)$$

In an actual measurement T would, of course, be finite, as a result of which the spectral resolution would be limited to 1/T. The temporal spectrum $\Phi_{\eta\eta}^{(U)}(y,\omega)$ cannot, in general, be expressed in terms of the spatial spectrum $S_{\eta\eta}(K)$. This can be done,

however, approximately for fast tow speeds, in which case the following asymptotic result is obtained [1]:

$$\Phi_{\eta\eta}^{(U)}(\omega,y) \sim \frac{1}{\omega} \int_0^{\pi/2} d\beta\, I(\omega U^{-1}\sec\beta)\,(1 - \exp - 2y\omega U^{-1}\sec\beta) \quad , \qquad (18)$$

where I is the excitation function entering in the definition of the spatial spectrum in (1). Equation (18) holds for U much greater than the group velocity of the internal wave motion (fast tow speed approximation). In addition, (18) is not valid for ω at and below the maximum Väisälä frequency. When (18) is evaluated at $\omega = KU$, one obtains

$$\Phi_{\eta\eta}^{(U)}(KU,y) \sim \frac{1}{U} \int_0^{\pi/2} d\beta\, \frac{I(K\sec\beta)}{K}\,(1 - \exp{-2Ky\sec\beta}) . \qquad (19)$$

Apart from a constant factor, (19) is identical to the spatial spectrum along a typical "cut" through the isotropic internal wave field. In [3] and [4] the form of I(K) is inferred from plots of $\Phi_{\eta\eta}^{(U)}(KU,y)$ as a function of K at various depths y. In general, the determination of I(K) would require solving the integral equation in terms of the given data. If, however, I(K) is *assumed* to obey a power law, viz., (7), then (19) becomes

$$\Phi_{\eta\eta}^{(U)}(KU,y) \sim \frac{C_p K^{-p-1}}{U} \int_0^{\pi/2} \cos^p\beta\,[1 - \exp{-2Ky\sec\beta}]\, d\beta \quad . \qquad (20)$$

For sufficiently large depths, viz., when

$$2Ky >> 1, \qquad (21)$$

the exponential term in the integrand may be dropped, while

$$\int_0^{\pi/2} \cos^p \beta d\beta = \frac{\sqrt{\pi}}{2} \frac{\Gamma\left(\frac{p+1}{2}\right)}{\Gamma\left(\frac{p+2}{2}\right)} \quad .$$

Consequently, the towed spectrum becomes

$$U\Phi_{\eta\eta}^{(U)}(KU,y) \sim \frac{\sqrt{\pi}}{2} \frac{\Gamma\left(\frac{p+1}{2}\right)}{\Gamma\left(\frac{p+2}{2}\right)} C_p K^{-p-1} \quad . \tag{22}$$

permitting the empirical determination of C_p and p from $\Phi_{\eta\eta}^{(U)}(KU,y)$.

IV. MAGNETIC FIELD COMPONENT AND GRADIENT SPECTRA OBSERVED FROM AIRBORNE MEASUREMENT PLATFORMS

We assume a platform moving with velocity V m/sec at a fixed height of y above the ocean surface (Fig. 2). The geomagnetic field is in the xy plane. Its direction with respect to the horizontal plane (sea surface) is defined by the angle ϕ_D (dip angle). The motion of the platform is parallel to $\underline{\ell}_1$, which is oriented at an angle α with respect to the vertical plane containing the geomagnetic field. The components of the magnetic field induced by internal waves are resolved along the mutually perpendicular directions $\underline{\ell}_1$, $\underline{\ell}_2$, $\underline{\ell}_3$, which may be considered fixed with respect to the platform. The temporal cross-spectrum of magnetic field components B_ν, B_μ will be denoted by $S_{\nu\mu}$. A typical component of the magnetic field gradient, $G_{\nu\mu}$, is defined as the derivative of B_μ with respect to direction ν. The gradient components are symmetrical, i.e., $G_{\nu\mu} = G_{\mu\nu}$. The temporal cross spectra of the gradients are denoted by $S_{\nu\mu;\nu\mu}$.

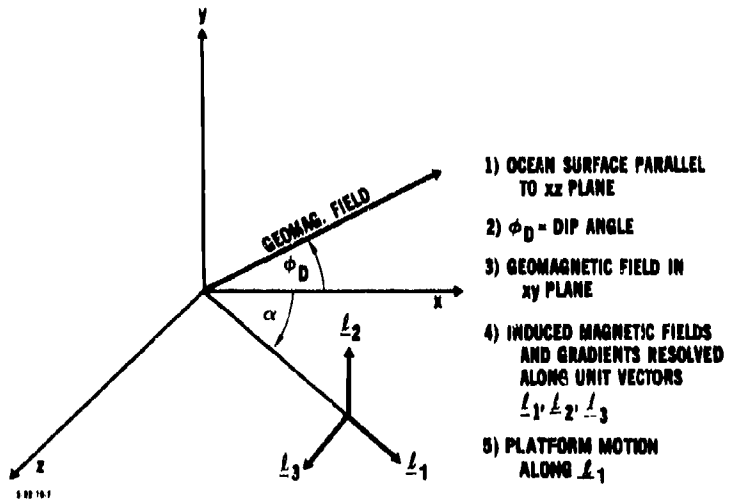

FIGURE 2

For frequencies above the maximum Väisälä frequency, the magnetic field and gradient spectra can be approximated by the following asymptotic expressions [1] (large tow speed approximation):

$$S_{\nu\mu}(\omega,y) \sim \frac{(\sigma\mu_o B)^2 C_p}{2(1+3\cos^2\phi_D)\omega} \int_0^{\pi/2} d\beta\, \tilde{g}_{\nu\mu}(\alpha,\beta)\, K^{-p+1} e^{-2Ky} \int_{-\infty}^{0} y'^2 N^2(y') e^{2Ky'} dy' \quad , \tag{23}$$

$$S_{\nu\mu;\nu\mu}(\omega,y) \sim \frac{C_p(\sigma\mu_o B)^2}{(1+3\cos^2\phi_D)\omega} \int_0^{\pi/2} d\beta\, \tilde{g}_{\nu\mu;\nu\mu}(\alpha,\beta)\, K^{-p+3} e^{-2Ky} \int_{-\infty}^{0} y'^2 N^2(y') e^{2Ky'} dy' \quad , \tag{24}$$

where y is the height above the ocean in meters, $K = \omega/(V\cos\beta)$, $\sigma = 4$ mho/m, $\mu_o = 4\pi \times 10^{-7}$ h/m, $B = 6.24 \times 10^7$ pT and the constant C_p has dimensions of $(\text{meters})^{2-p}$. The quantities $\tilde{g}$ in the integrands are dimensionless trigonometric polynomials, defined on page A-14. The spectra in (23) and (24) have dimensions of $(\text{pT})^2/\text{Hz}$ and $(\text{pT/m})^2/\text{Hz}$, respectively. The internal wave vertical displacement spectrum associated with the magnetic field spectra in (23) and (24) is given by (20). As noted earlier, according to the equipartition hypothesis, the latter is independent of N(y). On the other hand, the magnetic fields are seen to depend explicitly on N(y). (C.f. Eqs. 3-5.)

The computer program described in the Appendix is capable of providing magnetic field and gradient spectra for an arbitrary set of parameters and Väisälä frequency profiles. The N(y) profile input data can be supplied either analytically or as a set of values of N(y) spanning a specified depth below the ocean surface. Below this depth an exponential decay law is assumed. The constants C_p and p are to be supplied with the data.

Representative results obtained with the aid of the INTWAVE computer program are plotted in Figs. 3-8. The direction of platform motion α (defined in Fig. 2), platform velocity V (m/sec), height above the ocean surface Y (m), the magnetic dip angle, ϕ_D, and the exponent p governing the decay of the wave number spectrum (Eq. 7) are shown in each figure. The spectra are in $(pT/m)^2/Hz$, the horizontal scale is in Hz, and the subscripts pertaining to the gradient components conform to the coordinate system $\underline{\ell}_1$, $\underline{\ell}_2$, $\underline{\ell}_3$, in Fig. 2.

Figure 3 shows the vertical-horizontal (along the track) gradient spectrum for the exponentially stratified ocean without a mixed layer. Figure 4 shows the spectrum for the same gradient component for the exponentially stratified ocean with a mixed layer (case 2, in Fig. 1). The differences between Fig. 3 and Fig. 4 are seen to be quite insignificant. Figure 5 shows the spectra of the three orthogonal gradient components for the STD data set. Although the functional form of the spectra is essentially the same as for the exponentially stratified ocean, the overall levels of the magnetic field gradients are substantially higher. This is, of course, to be expected, in view of the much higher peak Väisälä frequency in this case. Somewhat lower spectral values are obtained when the platform motion is oriented at 90 deg with respect to the plane of the geomagnetic field, as shown in Fig. 6. In Figs. 3-6 the dip angle is taken as zero (equatorial zone). A dramatic increase in level is obtained when the dip angle is taken as 90 deg (polar regions), as shown in Fig. 7 for the STD data set.

In Figs. 3-7 the platform velocity is 100 m/sec (typical aircraft speed). To illustrate the effect of platform velocity, Fig. 8 shows the vertical-horizontal (along-the-track) gradient spectrum for platform speeds of 100 m/sec and 10 m/sec.

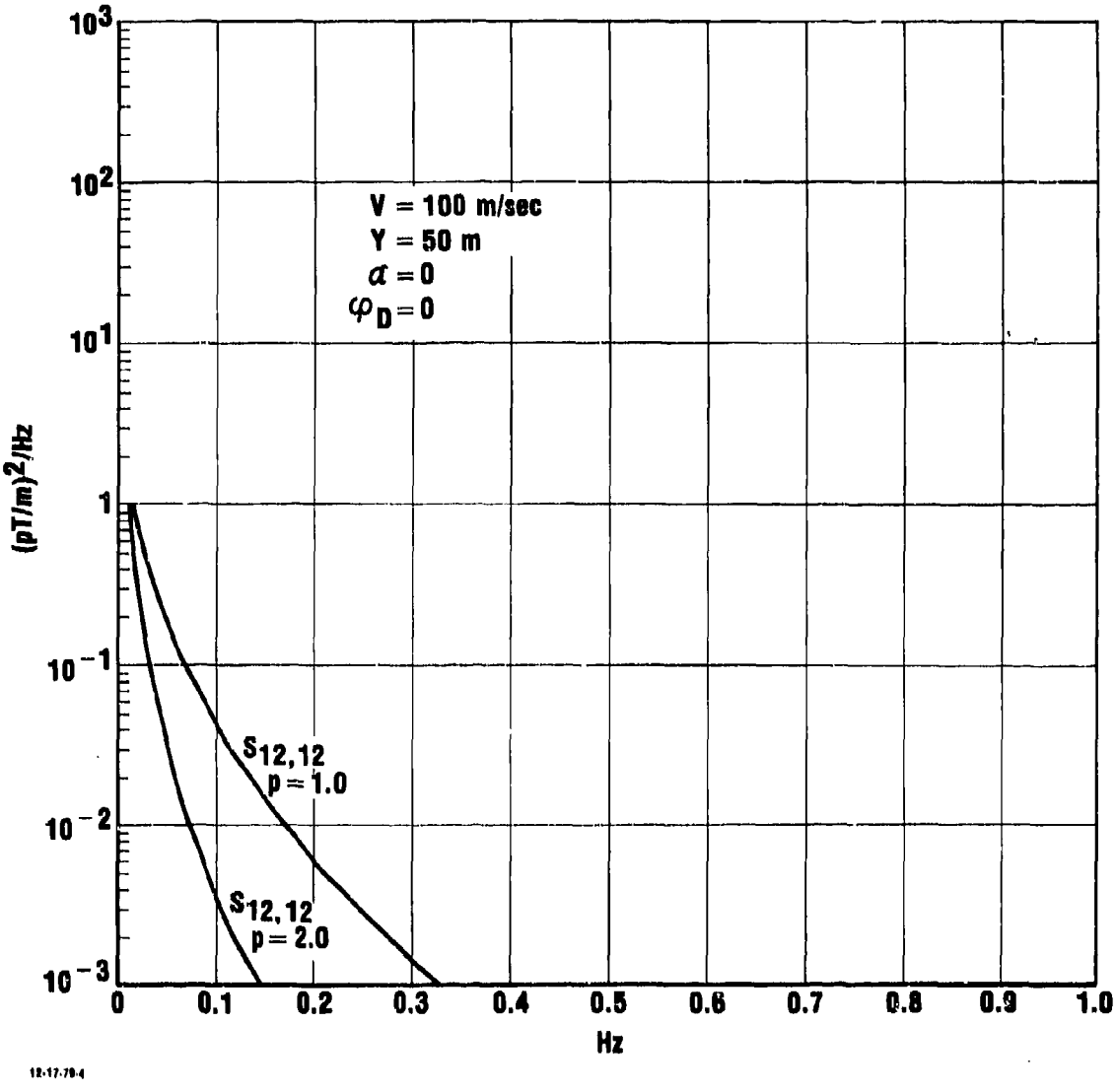

FIGURE 3. Internal Wave Induced Magnetic Field Gradient Spectra from a Moving Platform (exponentially stratified ocean)

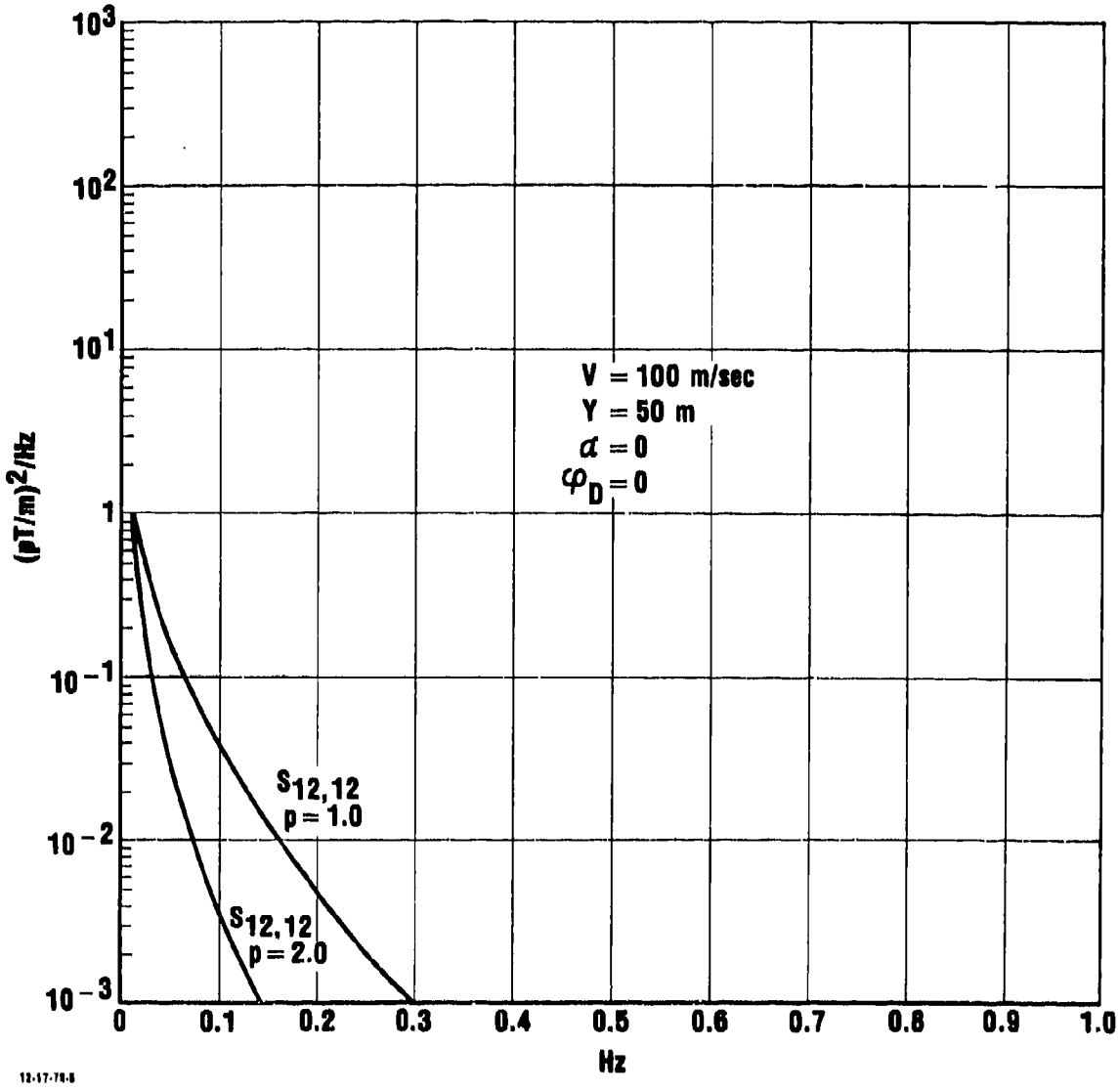

FIGURE 4. Internal Wave Induced Magnetic Field Gradient Spectra from a Moving Platform (exponentially stratified ocean with a mixed layer y_m = 50 meters)

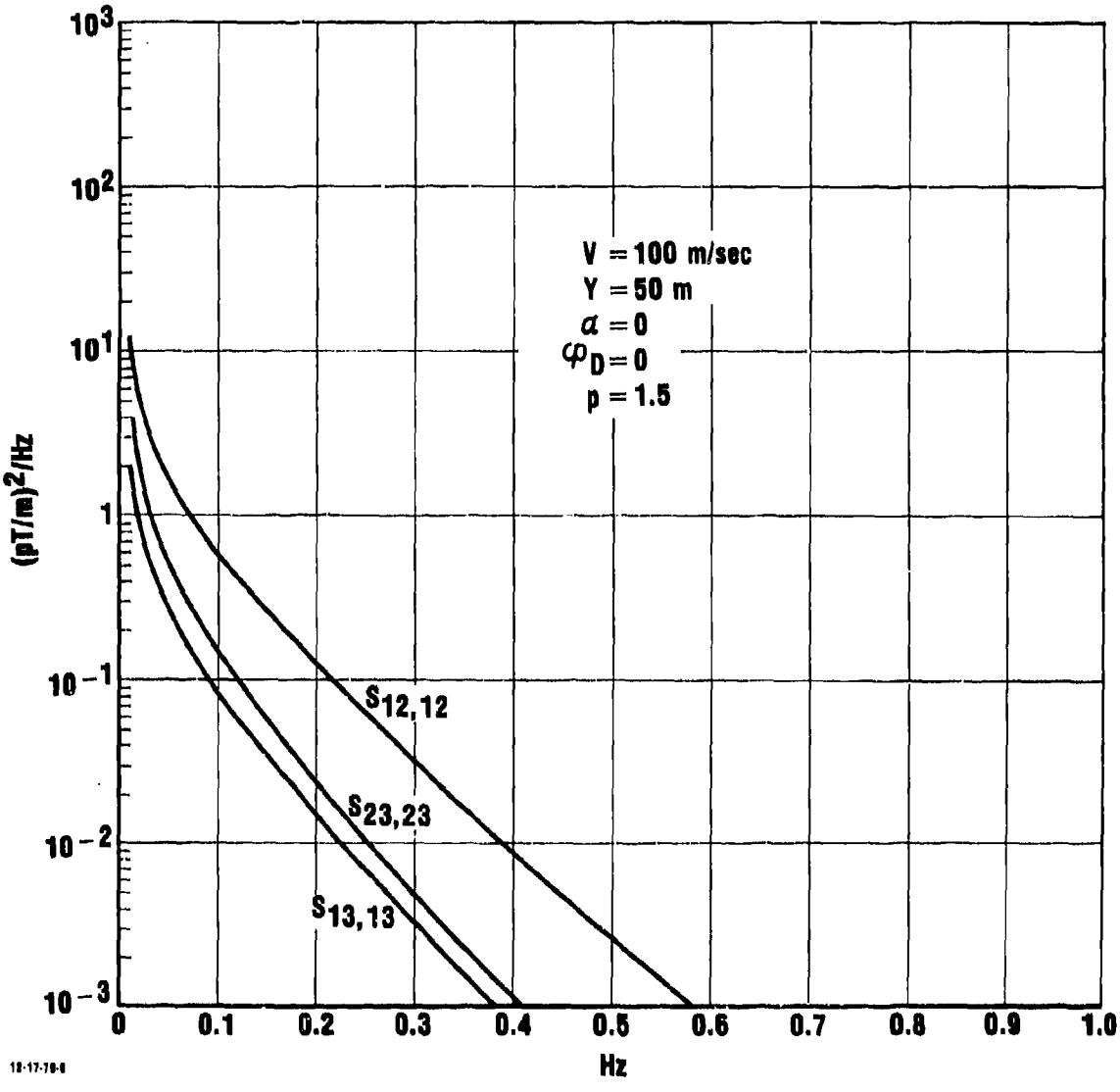

FIGURE 5. Internal Wave Induced Magnetic Field Gradient Spectra from a Moving Platform (STD Data Set)

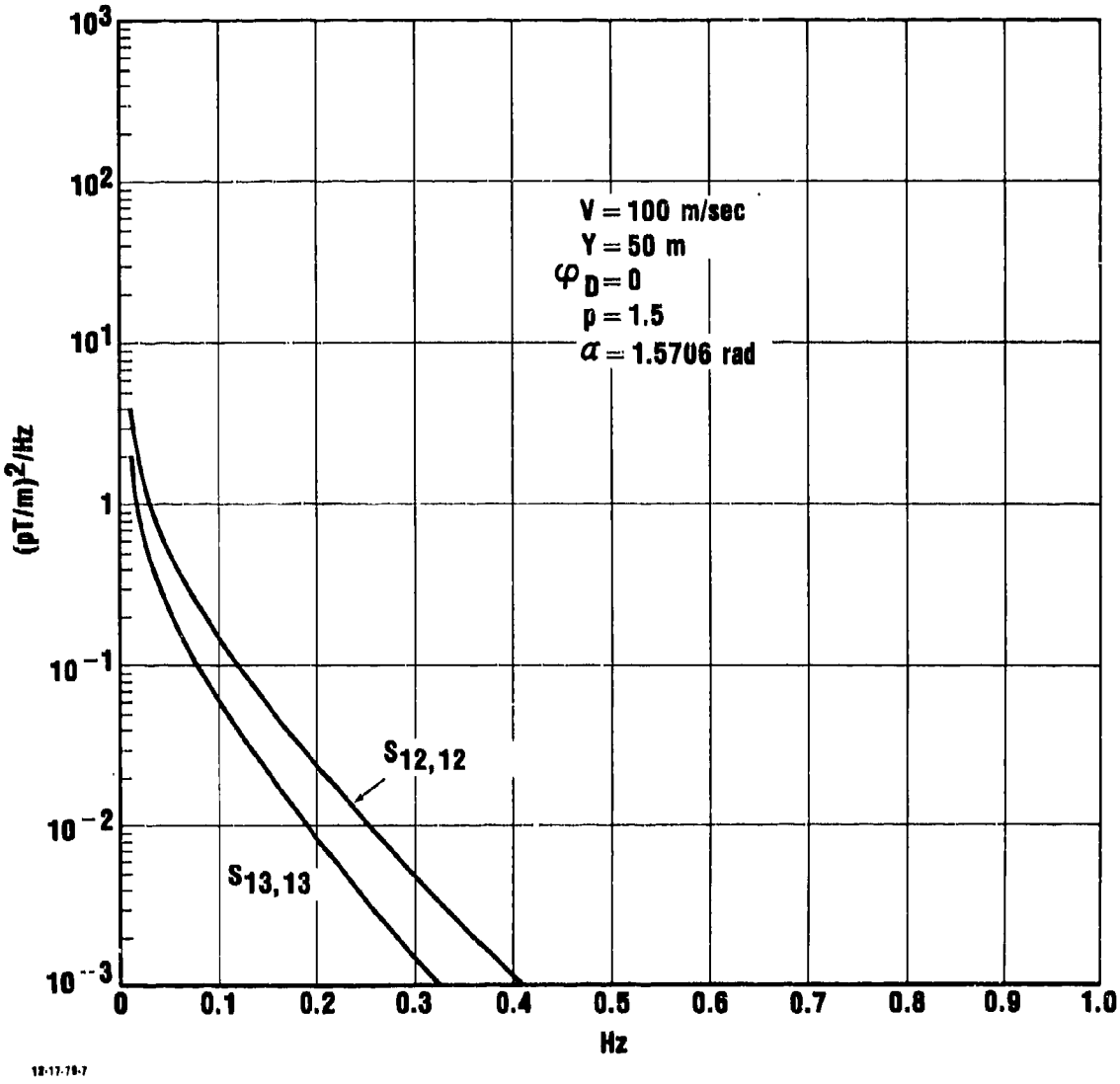

FIGURE 6. Internal Wave Induced Magnetic Field Gradient Spectra from a Moving Platform (STD Data Set)

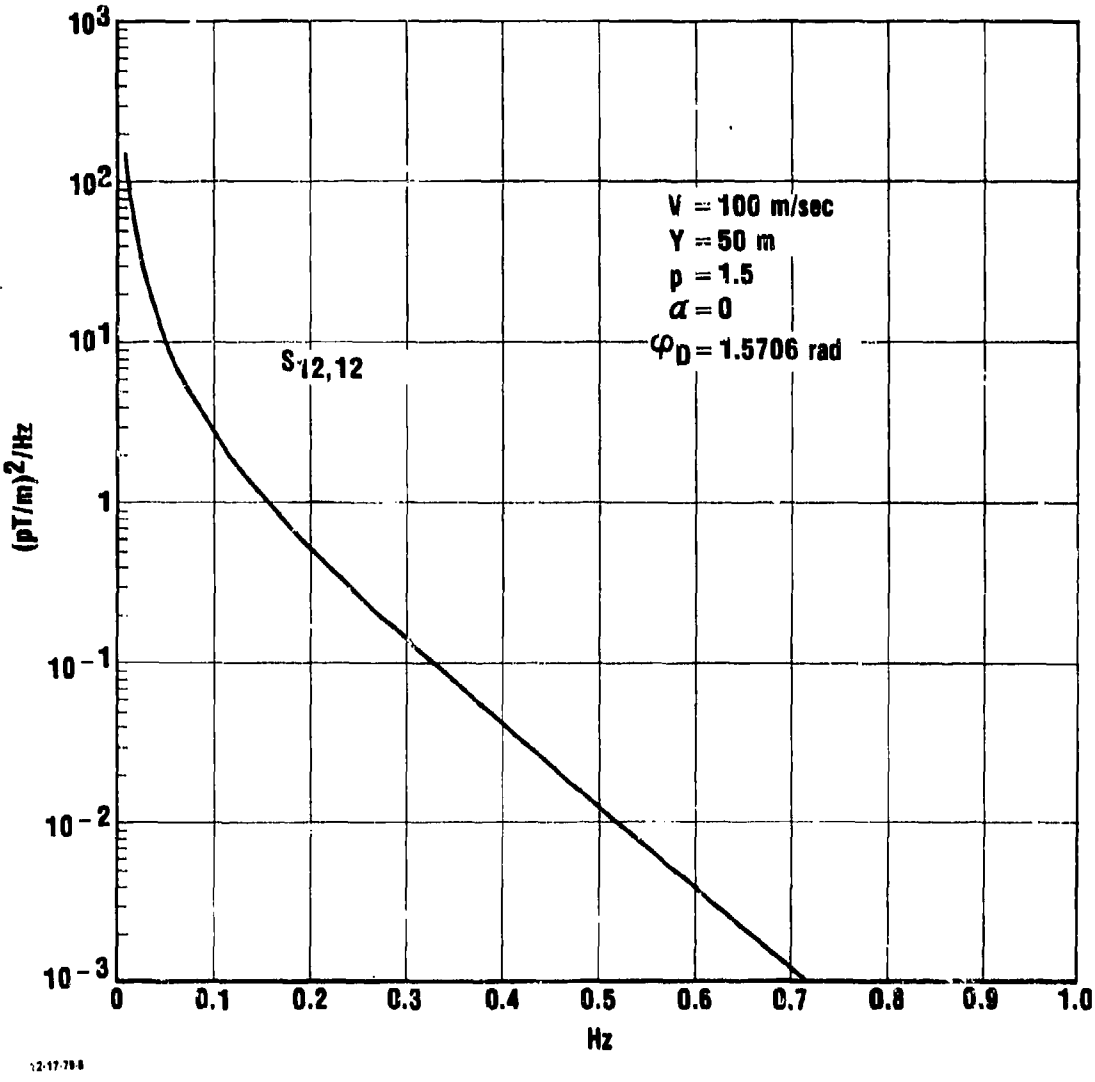

FIGURE 7. Internal Wave Induced Magnetic Field Gradient Spectra from a Moving Platform (STD Data Set)

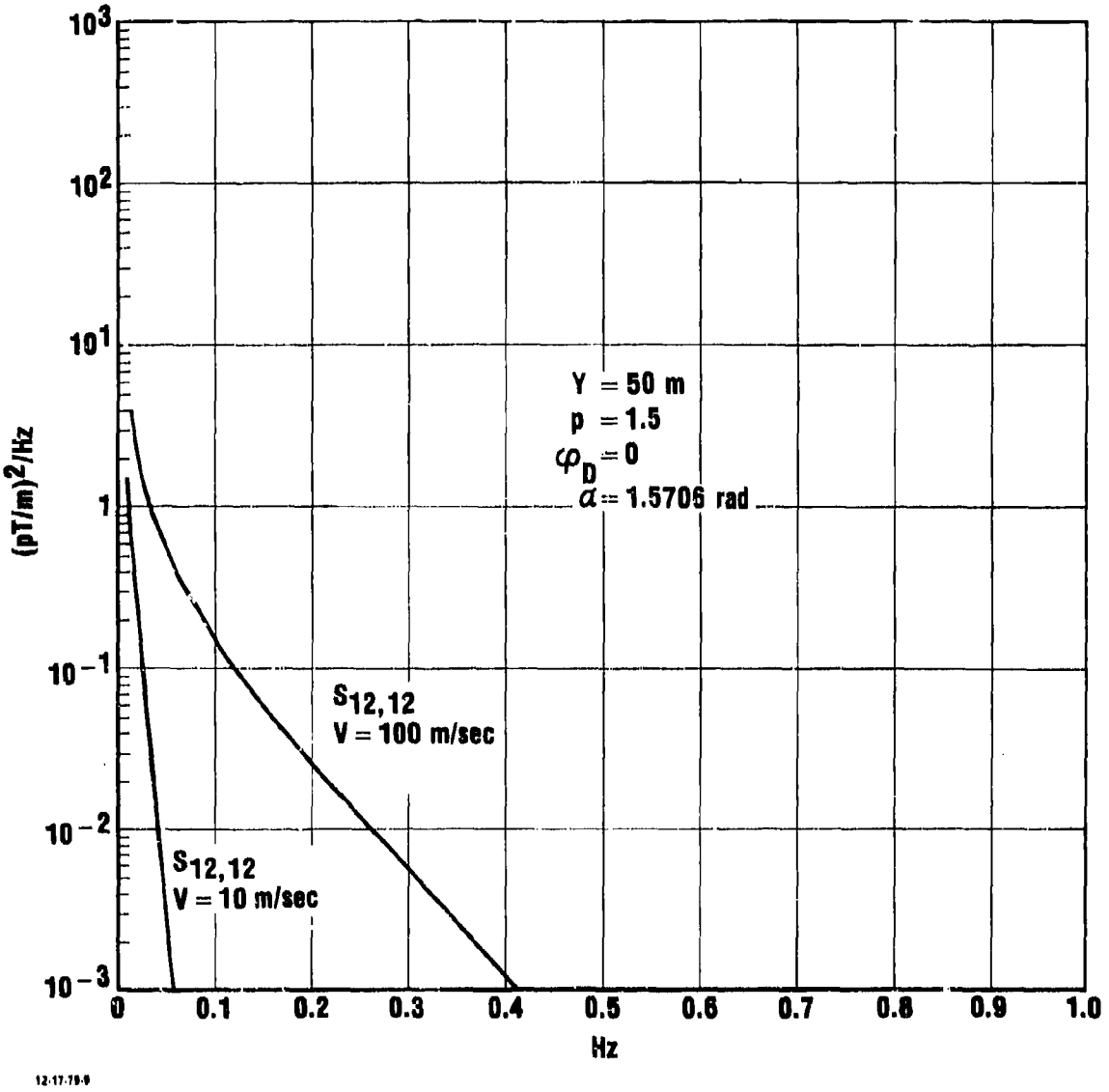

FIGURE 8. Internal Wave Induced Magnetic Field Gradient Spectra from a Moving Platform (STD Data Set)

V. CONCLUSIONS

A general conclusion that can be drawn from the results presented herein, as well as from the results of a large number of similar calculations using the INTWAVE program, is that internal wave induced magnetic field gradient spectra observed from a moving aircraft display no interesting structural features: all the spectra decrease monotonically with increasing frequency and are quite insensitive (both in regard to level and functional form) to the *spatial variation* in the Väisälä frequency profile. The critical parameters that affect the spectral level appear to be the area enclosed by the N(y) profile and the spatial wavenumber decay constant p, as well as the geomagnetic latitude.

APPENDIX

INTWAVE - A COMPUTER PROGRAM TO CALCULATE INTERNAL WAVE-INDUCED MAGNETIC FIELD SPECTRA

Elaine Marcuse

CONTENTS

ADDENDUMS

I. PURPOSE

The program INTWAVE was designed to calculate and plot the internal wave-induced magnetic field spectra (component and/or gradient) from a moving platform as a function of frequency. It provides for a choice among various assumptions as to the behaviour of the VÄISÄLÄ frequency vs. ocean depth.

II. EQUATIONS

The expression for the magnetic field component spectrum is given by Equation 255 of Reference 1. Rewritten in the notation of the INTWAVE program, the equation becomes:

$$S_{ij} \cong \frac{CONST1}{\omega} \int_0^{\pi/2} GC1(\beta) \left(\frac{\omega}{V\cos\beta}\right)^{-p+1} e^{-\frac{2\omega y}{V\cos\beta}} FN(\beta)\, d\beta \qquad (1)$$

where

$$CONST1 = \frac{49190}{1+3\cos^2\phi_D}, \qquad (2)$$

$$FN(\beta) = C_p \int_{-\infty}^{0} Y^2 N^2(Y)\, e^{\frac{2\omega Y}{V\cos\beta}}\, dY, \text{ and} \qquad (3)$$

$$GC1(\beta) = G_{ij}(\alpha+\beta-\pi) + G_{ij}(\alpha-\beta-\pi) \qquad (4)$$

The G_{ij} expressions (Equation 4) are a set of trigonometric polynomials defined for i,j = 1,3. These polynomials are given

in Addendum 1. The N(Y) in Equation 3 is the VÄISÄLÄ frequency for ocean depth Y, and C_p is an associated constant supplied with each N(Y) function.

Similarly, the expression for the magnetic field gradient spectrum, given by Equation 259 of Reference 1 becomes in the program notation

$$S_{k\ell mn} \approx \frac{2CONST1}{\omega} \int_0^{\pi/2} GC2(\beta) \left(\frac{\omega}{V\cos\beta}\right)^{-p+3} e^{-\frac{2\omega y}{V\cos\beta}} FN(\beta)\, d\beta \qquad (5)$$

where

CONST1 and FN(β) are defined as for Equation 1 and

$$GC2(\beta) = G_{k\ell mn}(\alpha+\beta-\pi) + G_{k\ell mn}(\alpha-\beta-\pi)$$

The $G_{k\ell mn}$ expressions of Equation 6 are a set of trigonometric polynomials defined for i,j,k = 1,3 and are listed in Addendum 1.

III. PARAMETERS

The parameters which are required for a particular calculation are as follows:*

1. V - platform velocity (m/sec)
2. y - height of platform above ocean surface (m)
3. α (Alpha) - angle between the direction of platform motion and the plane of the geomagnetic field (rad.) ($0 \leq \alpha \leq 2\pi$)
4. ϕ_D (PhiD) - magnetic dip angle (rad.) ($0 \leq \phi_D \leq \pi/2$)
5. i(ii) and j(jj) - directions of components of the induced magnetic field (i,j=1,3)

*The program name for each variable, when different, is given in parenthesis. In particular, all Greek letters are spelled out in the program.

6. k(kk), ℓ(ℓℓ), m(mm), n(nn) - the directions of gradients of the induced magnetic field (k,ℓ,m,n = 1,3; k<ℓ)
7. Ncase - an integer associated with each assumption about the VAISALA frequency vs. ocean depth (see Section IV) ($1 \leq Ncase \leq 4$)
8. p - the internal wave mode decay constant. For Ncase= 1,2, or 3, p = 1 or 2. For Ncase=4, p>0.
9. Y_m(YM) - this parameter is required only when Ncase= 2 or 3. It is the value of the depth at which the peak value of N(Y) occurs and is restricted to $0 < Y_m \leq 200m$

The calculations of S_{ij} and/or $S_{k\ell mn}$ are made as a function of ω (omega), over a range from $\omega = .02\pi$ to 2π, the values being more closely spaced at the low end and more widely spaced near 2ω. The actual spacing is given by $\omega/2\pi$ = .01(.01).1; .1(.02).2; .2(.025)1.00.

IV. THE VÄISÄLÄ FREQUENCY VS. DEPTH OF OCEAN

The function FN(β) in Equation 3 is dependent on the nature of the function N(Y), where Y is ocean depth (m), (Y<0) and N(Y) is the VÄISÄLÄ frequency for that depth. Several possible assumptions as to the nature of this relationship have been incorporated into the program, including one which is general in nature and can accept user supplied data points. They all contain a parameter b which is the reciprocal of the VÄISÄLÄ frequency asymptotic decay constant. In the program, at present the value of b is set at 1300 meters, but could easily be changed.

The four different assumptions which the program is designed to handle, indicated by the value of the input parameter Ncase, are as follows:

1. Ncase = 1 assumes an exponentially stratified ocean given by

$$N(Y) = N_m \, e^{Y/b} \qquad (7)$$

When this is substituted in Equation 3 and the resulting expressions integrated, we obtain

$$FN(\beta) = K_p \left\{ \frac{\cos\beta}{\cos\beta + \frac{\omega b}{V}} \right\}^3 \qquad (8)$$

where

$K_1 = .2169b$

$K_2 = .1832$

2. Ncase=2 assumes an exponentially stratified ocean with a mixed layer. N(Y) is defined by:

$$\begin{aligned} N(Y) &= 0 && , -Y_m \leq Y < 0 \\ N(Y) &= N_m e^{(Y+Y_m)/b} && , Y < -Y_m \end{aligned} \qquad (9)$$

The value of Y_m is user supplied.

Substituting this expression in Equation 3, and integrating the result yields

$$N(\beta) = K_p \cdot e^{\frac{-2\omega Y_m}{V\cos\beta}} \cdot f(\beta) \cdot \left\{ 2\left(\frac{Y_m}{b}\right)^2 + 2\left(\frac{Y_m}{b}\right) f(\beta) + f^2(\beta) \right\} \qquad (10)$$

where

$$f(\beta) = \frac{\cos\beta}{\cos\beta + \frac{\omega b}{V}}$$

$$K_1 = \frac{.3040b}{VINT2(Y_m,1)} , \quad K_2 = \frac{.3040}{VINT2(Y_m,2)} , \text{ and}$$

$$VINT2(Y_m,p) = \int_{V_c}^{\infty} V^{-p-1} \left[1 - \frac{e^{-2Y_m V/b}}{1+V} \right] dV \qquad (11)$$

where

$V_c = .3267$

The values of $VINT2(Y_m,p)$ were computed by Gaussian numerical quadrature for p=1, and for $Y_m = 0(25)200$. The results were such that linear interpolation for Y_m is adequate.

3. Ncase=3 assumes a thermocline with a well-defined peak at Y_m. N(Y) is given by:

$$N(Y) = Nm\left(\frac{-Y}{Y_m}\right)^{Y_m/b} e^{(Y+Y_m)/b} \qquad (12)$$

Integrating the resulting expression for FN(β) yields

$$FN(\beta) = K_p \cdot \left(\frac{2Y_m}{b} + 2\right)\left(\frac{2Y_m}{b} + 1\right)\left\{\frac{\cos\beta}{\cos\beta+\frac{\omega b}{V}}\right\}^{\left(\frac{2Y_m}{b} + 3\right)} \qquad (13)$$

where

$$K_1 = \frac{.1520b}{VINT3(Y_m,1)} \quad \text{and} \quad K_2 = \frac{.1520}{VINT3(Y_m,2)}$$

$$VINT3(Y_m,p) = \int_{V_c}^{\infty} V^{-p-1}\left\{1 - \frac{1}{(V+1)^{(2Y_m/b+1)}}\right\} dV \qquad (14)$$

The values of $VINT3(Y_m,p)$ were computed in the same way and for the same values of Y_m,p as for $VINT2(Y_m,p)$. Again linear interpolation for $0<Y_m\leq 200$ is adequate.

NOTE: If $Y_m=0$, the previous three cases become identical. For cases 2 and 3, a user supplied value of $Y_m\leq 200$ should be supplied.

4. Ncase=4. This is the most general case in that the N(Y) vs. depth relationship up to some maximum depth of YMIN is described by a user supplied set of up to 100 data points.* For depths below YMIN, an exponential relationship is assumed.

A set of NPT pairs of points NVAL, YVAL from depth of 0 to depth YMIN is supplied where $NVAL=N(Y)/N_m$, so that $0\leq NVAL\leq 1$.

*This limit on the number of data points could easily be changed if more points were necessary.

and YVAL=depth, so that $0 \geq YVAL \geq YMIN$. Since any value of N(Y) for Y>YMIN is obtained by linear interpolation in this set of points, it should be noted that the points should (if obtained from a curve) be chosen in such a way that linear interpolation is satisfactory, i.e., points should be more closely spaced where curvature is greatest and should include all minima and maxima. If YVAL = NMIN at Y = YMIN, the exponential expression used for N(Y) below depth YMIN is

$$N(Y) = N_m \, NMIN \, e^{(Y-YMIN)/b} \tag{15}$$

The expression for FN(β) for Ncase=4 becomes

$$FN(\beta) = C_p \left\{ \int_{YMIN}^{0} Y^2 N^2(Y) e^{\frac{2\omega Y}{V\cos\beta}} \, dY + \frac{N_m^2 NMIN^2 e^{\frac{2\omega YMIN}{V\cos\beta}}}{a^3} \left[(aYMIN-1)^2 + 1 \right] \right\} \tag{16}$$

where

$$a = 2\left(\frac{1}{b} + \frac{\omega}{V\cos\beta}\right)$$

The integral from Y = YMIN to 0 is obtained by numerical integration (Gaussian quadrature formula).

In using Ncase=4, along with the set of data points YVAL, NVAL, the set of parameters Nset (an identifier), NPT, Nm, NMIN, YMIN, and C_p must all be supplied by the user. For Nset=1, a set of STD data points and parameters has been used, the values of which are given in Addendum 2.

V. NUMERICAL QUADRATURE

A. THE S_{ij}, $S_{k\ell mn}$ INTEGRATION

The integration indicated by Equations 1 and 5 is performed in this program by using SIMPSON's rule as follows. The integral is obtained by using the statement

INT = SIMP2(BEGIN,END,ACC,NN,FUNCT,NN1,ACC1)

where the input parameters are

FUNCTN	-	The integrand, defined in a function subroutine
BEGIN	-	The beginning of the interval of integration (=0)
END	-	The end of the interval of integration (=π/2)
ACC	-	The accuracy desired in the result (=.0001)
NN	-	The maximum number of intevals into which the interval is to be subdivided before terminating the iteration (=1000)

and the outputs are

NN1	-	Actual number of intervals before iteration was terminated
ACC1	-	Relative accuracy* achieved in final estimate
INT	-	The final estimate of the value of the integral

*If the final estimate is AREA2 and the previous estimate is AREA1, the relative accuracy is defined as $\frac{AREA2-AREA1}{AREA1}$

An initial estimate of the integral is obtained by using four intervals and then the number of intervals is successively doubled until either NN1>NN or ACC1≤ACC.

In actual use for many combinations of parameter inputs, it was found that in most cases only 16 or 32 intervals were required to achieve accuracy of .0001.

B. INTEGRAL IN FN(β) for Case 4

The integral in Equation 16 must be obtained by numerical quadrature since N(Y) vs. Y is given by a tabular set of values, linear interpolation being used to obtain intermediary values. An attempt to get accuracy of .0001 with SIMPSON's rule required on the order of 2000-8000 points per integration; therefore, the Gauss method of numerical integration (in which the points of subdivision are not equally spaced, but chosen to give greater accuracy) was substituted using 96 points.

VI. INPUT CARD DECK

This section provides the information needed to supply an input deck required for a computer run of INTWAVE.

With the exception of the YVAL, NVAL set of data points supplied when Ncase=4, all inputs are members of a NAMELIST group, and can thus be given values by means of a NAMELIST input card in an unformatted manner, the details of which are given in Addendum 3.

a. The three NAMELISTS which contain all the required inputs are:

1. OPTIONS namelist. This is a group of five option parameters which are to be set equal to 0 or 1. The non-zero ones must be defined on the OPTIONS card. The parameters are:

(a) IPRINT. This is set=1 when an extra printout is desired of 17 equally spaced values of the integrand (from $\beta = 0$ to $\beta = \pi/2$) of Equations 1 and 5. This is normally used only in a debug run.

(b) ICALCG. This is set=1 if values of the component spectrum (S_{ij}) are to be calculated.

(c) ICALCC. This is set=1 if values of the gradient spectrum ($S_{k\ell mn}$) are to be calculated.

(d) IPLOTC. This is set=1 if plots of the component spectrum (S_{ij}) are to be produced.

(e) IPLOTG. This is set=1 if plots of the gradient spectrum ($S_{k\ell mn}$) are to be produced.

WARNING NOTES. Plots of either type cannot be produced unless the corresponding calculations are made, whereas the inverse is not true. Thus, the combination ICALCG=0, IPLOTG=1 is not a feasible one. Also when IPRINT=1, all six subscripts ii to nn must be assigned non-zero values.

2. PARAMS namelist. This group contains all the parameters listed in Section III, namely V, y, α, ϕ_D, p, Ncase, Y_m, and the six subscripts ii to nn.

   (a) Of these inputs Ncase and the six subscripts are integers; the others should have a decimal point included in their value.

   (b) Y_m is needed only if Ncase = 2 or 3.

   (c) The subscripts ii,jj are needed only if ICALCC=1 or IPRINT=1.

   (d) The subscripts kk, $\ell\ell$, mm, nn are needed only if ICALCG=1 or IPRINT=1.

   (e) Any parameter omitted from the PARAM card will be assigned a value 0, unless it follows a previous PARAM card in which case its value will remain unchanged.

3. CASE4 namelist. This set of inputs is required only when Ncase=4 on the PARAM card preceding it. It contains values for the following variables, all of which are associated with the set of N(Y) data points supplied.

   (a) Nset. This is an integer number assigned to each set of data points to uniquely identify it.

   (b) NPT. The number of data points supplied for the arrays NVAL, YVAL.

   (c) NMIN. The value of $N(Y)/N_m$ at depth YMIN.

   (d) YMIN. The last tabulated depth value (a negative number).

(e) N_m. The maximum value of N(Y).

(f) C_p.

NOTE: Only the first two of these five variables are integers.

b. CASE4 Data Points. The CASE4 namelist input card must be immediately followed by a set of data cards which provide a set of NPT values for the NVAL, YVAL arrays. The first set of values should be for Y=0 and the last set for Y=YMIN. The array of positive numbers - YVAL is punched on the input cards and converted in the program to negative values. The format in which these cards are to be punched is as follows:

1. Each pair of values NVAL, YVAL occupies a field of 10 columns, the first five for NVAL, the second five for YVAL.
2. The number may be placed anywhere within the 5-column field as long as the decimal point is included.
3. Eight pairs of values are included on each card, until all values are punched.

c. Varying Parameters Within One Run. A complete input deck for one run with one parameter set consists of an OPTIONS card followed by a PARAMS card, followed, if Ncase=4, by a CASE4 card and associated NVAL,YVAL cards, all terminated by an end-of-file card.

Results may be obtained for various parameter sets within one run by following the first sequence of input cards by a string of PARAM cards before the end-of-file card.

Everytime a calculation is completed, the next PARAM card in the input deck is read (until the end-of-file is reached). Any variables on the new PARAM card will have the new values assigned to them, all other variables will retain their previous value and the entire calculation is repeated. The number of plots which might be produced by such a run is equal to the number of PARAM cards in the input deck.

NOTE: Only one set of data points for Ncase=4 can be used within a given run, and the CASE4 card and associated NVAL, YVAL data cards need only be supplied once - after the first PARAM card which contains Ncase=4.

VII. OUTPUT

1. Printout

   a. If Ncase=4, the values of the CASE4 variables and the associated table of $N(Y)/N_m$ vs. depth values is printed.

   b. For each parameter set the values of all variables in the PARAM namelist group is printed.

   c. For each parameter set, a table of output values follows, giving for each of 47 values of ω:

      (1) The value of ω.

      (2) The value of the integrand INT1 = $S_{ij} \cdot \omega$/CONST1.

      (3) NPT1 = the number of intervals required to obtain the integral INT1.

      (4) ACC1 = the relative accuracy achieved in the SIMPSON integration INT1.

      (5) The value of S_{ij}*. The column is headed by the notation REAL or IMAG according to whether the values are real or imaginary.

      NOTE: If ICALCC=0, the above values will all be zero.

      (6) The value of the integrand INT2 = $S_{k\ell mn} \cdot \omega$/2CONST1.

      (7) NPT2 = number of intervals required to obtain the integral INT2.

      (8) ACC2 - the relative accuracy achieved in the SIMPSON integration INT2.

      (9) The value of $S_{k\ell mn}$*. The notation REAL or IMAG indicates whether the values are real or imaginary.

      NOTE: If ICALCC=0, the four preceding values will all be zero.

---

*The values of S_{ij} and $S_{k\ell mn}$ decrease as frequency ($\omega/2\pi$) increases. There is a cutoff value VALMIN such that once the spectrum being calculated is less than VALMIN, the computation for the spectrum ceases. The value is now set at $(10)^{-3}$, but could easily be changed.

The main reason for printing the NPT, ACC figures was to check on the behaviour of the function. If an output appeared with NPT1 or NPT2 = 512, it would indicate that the accuracy requested had not been reached and the iteration had terminated because doubling the number of intervals would exceed the limit of 1000. In this case, further examination would be indicated to see if some error had been introduced.

2. Plots

When the plot option is used, each run will produce either one or two plots for each parameter set in the run (S_{ij} or $S_{k\ell mn}$ or both). The plot is 10" by 10" on 6-cycle log paper the abscissa being frequency ($\omega/2\pi$=hz) which varies from 0 to 1. The ordinate scale is chosen in such a way that the maximum computed value of the function (S_{ij} or $S_{k\ell mn}$) will be included on the plot, but in no case are values of the ordinate less than $(10)^{-3}$ plotted. Each plot is labeled completely with the values of all the parameters, plus an alphanumeric description of the VÄISÄLÄ frequency assumption used.

ADDENDUM 1

THE G_{ij}, $G_{k\ell mn}$ TRIGONOMETRIC POLYNOMIALS

Let*

$$\lambda(w,\phi_D) = \cos^2 w \cos^2\phi_D + \sin^2\phi_D$$

Then the G_{ij} functions are defined by:

$$G_{11}(w) = \tfrac{1}{4}\cos^2(w-\alpha)\,\lambda(w,\phi_D)$$

$$G_{22}(w) = \tfrac{1}{4}\,\lambda(w,\phi_D)$$

$$G_{33}(w) = \tfrac{1}{4}\sin^2(w-\alpha)\,\lambda(w,\phi_D)$$

$$G_{12} = G_{21}(w) = \tfrac{i}{4}\cos(w-\alpha)\,\lambda(w,\phi_D)$$

$$G_{13} = G_{31}(w) = \tfrac{1}{4}\cos(w-\alpha)\sin(w-\alpha)\,\lambda(w,\phi_D)$$

$$G_{32}(w) = G_{23}(w) = \tfrac{i}{4}\sin(w-\alpha)\,\lambda(w,\phi_D)$$

and the $G_{k\ell mn}$ functions by:

$$G_{1212}(w) = \tfrac{1}{8}\cos^2(w-\alpha)\,\lambda(w,\phi_D) = \tfrac{1}{2}G_{11}(w)$$

$$G_{1313}(w) = \tfrac{1}{32}\sin^2 2(w-\alpha)\,\lambda(w,\phi_D) = \tfrac{1}{8}\sin^2 2(w-\alpha)\,G_{22}(w)$$

$$G_{2323}(w) = \tfrac{1}{8}\sin^2(w-\alpha)\,\lambda(w,\phi_D) = \tfrac{1}{2}G_{33}(w)$$

$$G_{1223}(w) = \tfrac{1}{8}\sin(w-\alpha)\cos(w-\alpha)\,\lambda(w,\phi_D) = \tfrac{1}{2}\sin(w-\alpha)\,G_{12}(w)/i$$

$$G_{1231}(w) = -\tfrac{i}{16}\sin 2(w-\alpha)\cos(w-\alpha)\,\lambda(w,\phi_D) = -\tfrac{1}{4}\sin 2(w-\alpha)G_{12}(w)$$

$$G_{2313}(w) = -\tfrac{i}{16}\sin 2(w-\alpha)\sin(w-\alpha)\,\lambda(w,\phi_D) = -\tfrac{1}{4}\sin 2(w-\alpha)G_{32}(w)$$

---

*The G_{ij} used here are denoted by the lower case letter in [1].

ADDENDUM 2

CASE 4, SET 1 PARAMETERS AND DATA POINTS

The STD data used for Ncase=4 runs was obtained from a curve of $N(Y)/N_m$ vs. Y (See Figure 1). Fifty points were selected from the curve in such a way that a good approximation to the curve could be obtained by connecting the points with straight lines. The pairs of values used are as follows:

n	N(Y)/Nm	-Y	n	N(Y)/Nm	-Y
1	.3	0	26	.880	65.0
2	.325	5.0	27	.882	70.0
3	.350	8.5	28	.880	73.0
4	.375	10.5	29	.875	75.0
5	.40	12.2	30	.870	77.0
6	.5	16.5	31	.855	80.0
7	.6	19.0	32	.810	85.0
8	.850	26.5	33	.770	90.0
9	.930	30.0	34	.730	94.0
10	.960	31.5	35	.700	98.0
11	.975	32.5	36	.625	110.0
12	.990	34.0	37	.560	120.0
13	.995	34.5	38	.500	130.0
14	1.0	36.7	39	.440	140.0
15	.990	39.0	40	.390	150.0
16	.980	40.0	41	.360	156.0
17	.965	42.0	42	.330	164.0
18	.950	44.0	43	.300	174.0
19	.930	47.5	44	.280	181.0
20	.915	50.0	45	.260	188.0
21	.910	51.0	46	.250	193.5
22	.900	52.5	47	.240	198.0
23	.890	56.0	48	.225	207.0
24	.885	57.5	49	.220	215.0
25	.880	62.0	50	.210	230.0

The parameters associated with this set of data points are:

Nset = 1
NPT = 50

$N_m = .02182$

NMIN = .21

YMIN = -230.

$C_p = .004756$

p = 1.5

so that for depth $Y < -230$, $N(Y) = (.02182)(.21)e^{(Y+230)/1300}$

ADDENDUM 3

NAMELIST INPUT CARDS*

When a group of variables is identified by a NAMELIST group name, input and output of these variables is possible using unformatted data cards in which any subset of the variables in the group may be assigned values as follows.

The card must contain a $ in Column 2 (Column 1 left blank) immediately followed by the NAMELIST group name with no embedded blanks. After that follows a string of data items of the form variable = constant, (Example: A=1.57, kk=5, CON = 22.3E-5) separated by commas, the last record terminating with a $ instead of a comma.

More than one card can be used to contain a NAMELIST input set provided that the first column of each card is left blank, and that each card except the first one ends with a constant followed by a comma.

To illustrate, if the following set of NAMELIST input cards were submitted for an INTWAVE run, with 7 data cards containing the 50 pairs of data points NVAL, YVAL, immediately after the CASE4 input card, the run would produce three plots:

1. For CASE4, Set 1 data with $\alpha = \phi_D = \phi$, V=100, Y=50, p=1.5
2. For CASE3 with Y_m=50, $\alpha = \pi/2$, $\phi_D = 0$, V=100, Y=50, p=1
3. Same as (2.) except that p=2.

*This description applies specifically to the CDC6400 computer using the NOS/BE operating system.

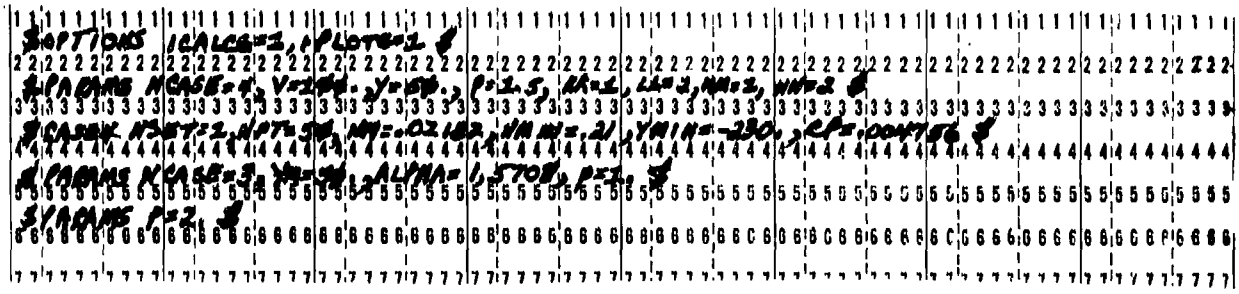

NOTE: On any PARAM card only those variables whose values are to be changed need be assigned values. The variables in the group which are not assigned values will be taken as zero, provided a CLEAR command is used in the control card deck.

ADDENDUM 4

CORRELATION COEFFICIENTS

The INTWAVE program can also be made to generate the following three sets of correlation coefficients:

$$\rho_{1231}(\omega) = \sqrt{\frac{|S_{1231}(\omega)|^2}{S_{1212}(\omega) \cdot S_{1313}(\omega)}} \quad ,$$

$$\rho_{1232}(\omega) = \sqrt{\frac{|S_{1232}(\omega)|^2}{S_{1212}(\omega) \cdot S_{2323}(\omega)}} \quad ,$$

$$\rho_{1323}(\omega) = \sqrt{\frac{|S_{2313}(\omega)|^2}{S_{2323}(\omega) \cdot S_{1313}(\omega)}} \quad ,$$

where the $S_{k\ell mn}$ quantities are defined by Equation 5, all parameters but the subscripts being kept constant over the set of calculations.

In order to compute these correlation coefficients in a run of INTWAVE, the run must be set up in the following way:

a. A new option parameter, ICORR must be added to the OPTIONS namelist input card, with value = 1. The value of ICALCG must also equal 1.

b. The first PARAMS namelist input card must define all the required parameters including one of the six sets of kℓmn subscripts required for the correlation coefficients.

c. The next five PARAM namelist input cards must change only the values of kk, ℓℓ, mm, and nn in any order such that the six required $S_{k\ell mn}$ arrays are calculated.

d. Correlations for other parameter combinations can follow the first set of calculations by repeating the entire sequence of six PARAM input cards, the first one in each set defining the changed parameter(s).

To illustrate, for one set of correlation coefficients, assume the first PARAM card contains ii=1, jj=2, kk=1, ℓℓ=2. Then a set of five PARAM cards which would produce the required arrays might be:

```
1. $PARAMS  LL=3, NN=3 $
2. $PARAMS  KK=2, MM=2 $
3. $PARAMS  MM=1$
4. $PARAMS  KK=1, LL=2, MM=3, NN=1 $
5. $PARAMS  NN=2 $
```

Note that since the $S_{k\ell mn}$ calculations were terminated when the values became less than VALMIN=10^{-3}, the correlation will be given as 0 if any of the spectrum values in the numerator < 10^{-3}. Also if any of the spectrum values in the denominator < 10^{-3}, the correlation value is undefined.

After the six required $S_{k\ell mn}$ arrays have been computed and printed, the correlation coefficients will be computed and printed for the 47 values of ω used - the table giving values of $\omega/2\pi$, $\rho_{1231}(\omega)$, $\rho_{1232}(\omega)$, and $\rho_{1323}(\omega)$.

REFERENCES

[1] W. Wasylkiwskyj, "Electromagnetic Fields Induced by Ocean Currents," IDA Paper P-1399, July 1979.

[2] C.J.R. Garrett and W.H. Munk, "Space-Time Scales of Internal Waves," *Geophys. Fluid. Dyn.*, 2, pp. 225-264, 1972a.

[3] D.M. Milder, "Partitioning of Energy, Vorticity and Strain in Upper-Ocean Internal Waves," Areté Associates, Santa Monica, California, August 1977.

[4] K.W. Nelson and D.M. Milder, "Internal Wave Displacement and Vertical Coherence Spectra from Towed Thermistor Chain Measurements in the Upper Thermocline," Areté Associates, Santa Monica, California, August 1977.